Generalized Distributed Multiple Turbo Coded Cooperative Differential Spatial Modulation

Jiangli Zeng[1*], Sanya Liu[2], and Hui Wang[3]
[1] College of Electronic and Information Engineering, Nanjing University of Aeronautics and Astronautics, No. 29, Jiangjun Road, Jiangning District, 211106 Nanjing, China
[e-mail: zengjiangli6856@nuaa.edu.cn]
[2] Dept. of Communication Engineering, Huaqiao University, 668 Jimei Road, 361021 Xiamen, China
[e-mail: sanya.liu.phd@hqu.edu.cn]
[3] Meteorological Equipment Information Room, Civil Aviation Wenzhou Air Traffic Control Station, 1 Longwan Airport Avenue, 325000 Wenzhou, China
[e-mail:chuanhui_yu@163.com]
[*]Corresponding author: Jiangli Zeng

Received May 6, 2022; revised January 21, 2023; accepted February 22, 2023; published March 31, 2023

Abstract

Differential spatial modulation uses the antenna index to transmit information, which improves the spectral efficiency, and completely bypasses any channel side information in the recommended setting. A generalized distributed multiple turbo coded-cooperative differential spatial modulation based on distributed multiple turbo code is put forward and its performances in Rayleigh fading channels is analyzed. The generalized distributed multiple turbo coded-cooperative differential spatial modulation scheme is a coded-cooperation communication scheme, in which we proposed a new joint parallel iterative decoding method. Moreover, the code matched interleaver is considered to be the best choice for the generalized multiple turbo coded-cooperative differential spatial modulation schemes, which is the key factor of turbo code. Monte Carlo simulated results show that the proposed cooperative differential spatial modulation scheme is better than the corresponding non-cooperative scheme over Rayleigh fading channels in multiple input and output communication system under the same conditions. In addition, the simulation results show that the code matched interleaver scheme gets a better diversity gain as compared to the random interleaver.

Keywords: generalized distributed multiple turbo code (GDMTC), joint parallel iterative decoding, code matched interleaver (CMI), Differential spatial modulation (DSM), multi-turbo codes, Multiple input and output (MIMO).

1. Introduction

Diversity techniques have been studied in literature in terms of time, frequency, spatial and other variants to overcome negative affect of channel weakens and the resulting decline in quality of service in wireless communication. Multiple input and output (MIMO) technology can be used to achieve diversity technology [1]. 5G wireless communication is expected to bring higher spectral efficiency and energy efficiency, various diversity techniques have been proposed to achieve these goals. The recently proposed Index Modulation (IM) technique has aroused great interest, which by selecting different index numbers to transmit information. Recently, IM is widely used in many communication systems. The paper [2] proposed a novel communication scheme, which utilize the IM technology in conveying orthogonal frequency division multiplexing (OFDM) bits. Monte Carlo simulations show it can achieve better transmission performance than classical OFDM schemes. A scheme called layered-OFDM with IM is proposed in literature [3]. In this scheme, all subcarriers are first divided into some layers, then the IM technology are used to transmit bits of every layer. The first attempt to apply IM concept to spatial domain was spatial modulation (SM) which provides high spectral efficiency [4]. As a transmission technology, SM can not only overcome the multipath interference problem, but also reduce the complexity while ensuring the data rate and performance [5]. There are many research findings of SM applied in different fields. In the paper [6], the author presented a new scheme that named generalized precoding-aided quadrature spatial modulation. It extends the traditional quadrature SM to the receiver side and the simulation show the scheme get a better performance than to the conventional generalized precoding-aided SM scheme in same spectral efficiency. This survey [7] not only provides a comprehensive overview of the latest research progress and achievements on SM technology, but also expounds the composite application of SM technology with other cutting-edge technologies, as well as its application in emerging communication systems.

Recently, a Differential Spatial Modulation scheme (DSM) is proposed that completely ignores any channel side information (CSI) at the transmit node or receive node, while retaining the properties of a single active transmit antenna [8]. DSM technique is part of MIMO antennas, which is developed based on the SM technology. It introduces the time dimension on the basis of the traditional SM technology and performs differential operations in the time domain, thereby completely avoid the complicated channel estimation process of the receiving end [9]. At the same time, DSM also maintains the advantages of SM. It only activates one antenna per time slots, so there is no need to achieve synchronization between antennas and there is no inter-channel interference. DSM has been carried out related research with channel code. In literature [10], the author proposes a gray code order for antenna index permutations for DSM. This paper [11] proposed a new communication system called the absolute amplitude differential phase SM on the basis of traditional amplitude PSK aided DSM scheme. Monte Carlo simulations shown the proposed scheme is tolerated more flawed information under the channel statistics.

In addition, cooperation technique can get higher data rates when compared to a non-cooperative communication system [12-13]. The literature [14] conceived the idea of user cooperation in the space-time domain, and proposed a distributed space-time code scheme which can make full use of the spatial diversity between cooperative users. Later, a slightly different system appeared in the literature [15], which is referred to as cooperation. A distributed code cooperative scheme with turbo code was firstly used in [16]. In addition, much research has been conducted on a wireless cooperative communication system using large-scale relay. This paper [17] proposed a novel DSM cooperative system scheme, which utilized

complementary codes at the transmitter to overcome the shortcomings of the conventional DSM cooperative system. Monte Carlo simulations shown the proposed scheme can upgrade the system transmission efficiency and avoid the channel interference.

Turbo code is a widely used and popular technique of channel code in recent years. Turbo codes show the best bit error ratio (BER) performance at low to moderate coding rates compared to LDPC code and polar code [18-19]. As one of the key techniques of commercial 3G mobile communication systems, various researches on turbo codes have also attracted the attention of many scholars [20]. Recently, many cooperative communication systems about Turbo codes have been proposed [16, 21]. Further, the interleaver is an important factor in the construction of turbo code, different interleavers have been reported in [22-23]. But the performance of interleaver has not been systematically evaluated in the coded-cooperative system. Therefore, interleaver is a key factor of turbo coded-cooperative system. At the same time, we consider code matched interleaver (CMI) as a better interleaver for enhancing the error performance of code cooperation system in the following proposed setup.

In the literature [24-25], a multi-turbo codes and a corresponding suitable decoder algorithm is proposed, which is analyzed a multi-turbo code and a corresponding suitable decoder analyzed from the approximation of the maximum a posteriori probability (MAP) decision rule. We find that the multi-turbo codes are naturally suitable for the cooperation communication system owing to the unique encoding and decoding structure of turbo code. Thus, we firstly apply the multi-turbo communication system to the construction of cooperative turbo code and propose a corresponding joint parallel iterative decoding for it, we introduced the DSM method to the communication scheme at the same time. Then, we proposed a generalized distributed multiple-turbo coded cooperative differential spatial modulation (GDMTC-DSM) scheme based on generalized distributed multiple turbo code (GDMTC) and DSM. The application of turbo code can significantly improve the bit error rate. At the same time, the application of information modulation and antenna index modulation improves the bandwidth efficiency of the entire communication scheme. In addition, the application of interleaver is a key factor affecting the BER of turbo code. Here we have studied CMI and considered it to be a better interleaver. We have also verified its performance in the coded cooperative communication scheme.

The main contributions of this paper can be depicted as follows:

1) The research about turbo code [26] and DSM [8] are all have a potential breakthrough to bring higher spectrum efficiency and energy efficiency. The turbo code scheme is applied to DSM combined with higher order modulation for the first time, which may provide a more high-speed and effective communication scheme in the future.
2) The GDMTC communication scheme and the corresponding joint parallel iterative decoding is proposed, which gets a better BER performance in cooperative scheme after verification.
3) The turbo code system and GDMTC system are effectively extended to coded-cooperative scheme scenario i.e. TC-DSM and GDMTC-DSM scheme. Monte Carlo simulations show that the proposed the performance of GMDTC-DSM scheme outperforms the corresponding non-cooperative TC-DSM scheme over Rayleigh fading channels in MIMO communication system under the same conditions.
4) The CMI is a new interleaver method in turbo code and it is employed for the first time to TC-DSM and GDMTC-DSM schemes, which get a better performance than random interleaver (RI) in cooperative DSM schemes after verification.

Section 2 briefly explain CMI theory. Section 3 proposes a TC-DSM scheme against cooperative scenario and presents its system model. Section 4 proposes a GDMTC-DSM

scheme and describes its system model. Section 5 presents the proposed joint parallel iterative decoding for GDMTC-DSM system. Section 6 presents the Monte Carlo experiment results with the proposed scheme on the Slow Rayleigh channel are given. In the end, the conclusion is list in Section 7.

2. The coded matched interlever

In the communication scheme based on turbo code cooperation, we focus on the design of so-called code-matched interleaver for the turbo codes, which can give an insight of the particular role of the interleaver within the individual parallel concatenated codes. The literature [12] introduces the details of CMI model.

The generator matrix of turbo code with two constituent RSC encoders is $G=[1,g_a(D)/g_b(D)]$, where $g_a(D)=1+D^2$ is a forward polynomial and $g_b(D)=1+D+D^2$ is a backward polynomial. Suppose m be original input information sequence for the first RSC encoder which generating the output sequence (m_1^2, p_1) . Simultaneously, let m_2^2 be the second interleaved sequence encoded by the second RSC encoder which generates another parity bit sequence p_2 .

Suppose ω to be the weight of the input sequence and as well let $\omega(p_1)$ and $\omega(p_2)$ be the weights of the interleaved parity sequences, respectively. Thus, the whole weight of the new generated code could be given as below

$$d=\omega+\omega(p_1)+\omega(p_2) \tag{1}$$

The weight-2 input sequence and the interleaved information can be represented by (2) and (3) respectively:

$$m_1^2=\left(1+D^{\alpha k_1}\right)D^{\beta_1} \tag{2}$$

$$m_2^2=\left(1+D^{\alpha k_2}\right)D^{\beta_2} \tag{3}$$

where k_1=1, 2, 3, … and k_2=1, 2, 3, … are positive integer, α is the minimum distance between "1"s in weight-2 sequence m_1^2 and m_2^2 respectively. β_1 and β_2 are time delay, β_1 =1, 2, 3, …as well as β_2 .

Let $Q_{\min}$ be the smallest parity information sequence generated from the weight-2 input information sequence. Thus, the weight of the generated sequence is shown as

$$k_j\left(Q_{\min}-2\right)+2 \tag{4}$$

where k_j=1, 2, 3, … and j=1,2. As a result of the input sequence with a weight-2, the entire weight of the generated codeword is expressed as

$$\begin{aligned} d&=2+k_1\left(Q_{\min}-2\right)+2+k_j\left(Q_{\min}-2\right)+2\\ &=6+\left(k_1+k_j\right)\left(Q_{\min}-2\right)\end{aligned} \tag{5}$$

Let i_1 and i_2 be the position of each '1' of an information sequence of weight-2 m_1^2 , and let i_2 be the position of each '1' after it interleaves, respectively. Suppose that the new 1's position is $\pi\left(i_1\right)$ and $\pi\left(i_2\right)$ shown in **Fig. 1**. If the position satisfied the detrimental case as follows

$$\left|P_1 - P_2\right| \bmod \alpha = 0 \text{ and } \left|\pi\left(P_1 - \pi\left(P_2\right)\right)\right| \bmod \alpha = 0 \tag{6}$$

under this situation, the mapping of interleaver will lead to a worse information sequence, because the spacing between the original and the interleaved sequence of two consecutive "1"s is a multiple of a. Thus, RSC 2 encoder will cause a low parity check weight $\omega\left(P_2\right)$ and then the whole weight of codeword will be lowered. For the purpose of avoiding this case, the interleaver should design to mapping condition such as

$$\left|P_1 - P_2\right| \bmod \alpha = 0 \left|\pi\left(P_1\right) - \pi\left(P_2\right)\right| \bmod \alpha \neq 0 \tag{7}$$

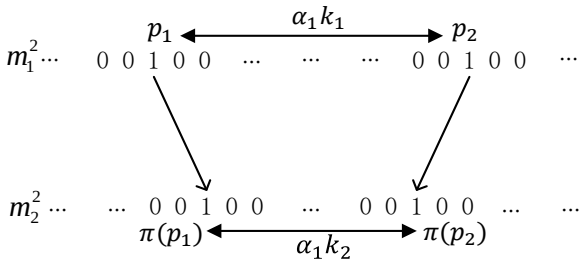

Fig. 1. A weight-2 input sequence mapped to same mode after interleaving.

But not all the weight-2 input codes satisfied (6) are worse. A threshold defined by a parameter in literature [12], which is given as follows

$$6 + (k_1 + k_2)(Q_{\min} - 2) \leq d_{\max}^{r=2}$$

$$(k_1 + k_2) \leq \frac{d_{\max}^{r=2} - 6}{(Q_{\min} - 2)} \tag{8}$$

The literature set forth how to design *S*-random interleaver. At the same time, an input sequences with weight-4 also may lead to compound error event (chain reaction of two single error events) is shown in Figure 2. Perform the same analogy on the weight-2 input sequence, the new weight generated by weight-4 input sequence m_1^4 can be shown:

$$d = 12 + \left(k_1^{'} + k_2^{'} + k_3^{'} + k_4^{'}\right)\left(Q_{\min} + 2\right) \tag{9}$$

Assume the positions of "1"s are represented by $P_1 < P_2 < P_3 < P_4$ for weight-4 input sequence m_1^4 where, as $P_1 < P_2 < P_3 < P_4$. After the information sequence m_1^4 passed through an interleaver to get a new interleaved sequence, thus the "1"s positions in the interleaved sequence are defined by $\pi(P_1), \pi(P_2), \pi(P_3)$ and $\pi(P_4)$ which is shown as **Fig. 2**.

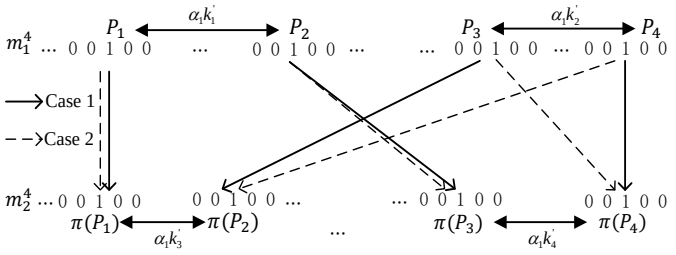

Fig. 2. A weight-4 input sequence mapped to same mode after interleaving

The worst result for weight-4 information sequence is shown as follows:

$$\begin{cases} \text{If } |P_1 - P_2| \bmod \alpha = 0 \text{ and } |P_3 - P_4| \bmod \alpha = 0 \\ \text{Then } |\pi(P_1) - \pi(P_3)| \bmod \alpha = 0 \\ \text{and } |\pi(P_2) - \pi(P_4)| \bmod \alpha = 0 \end{cases} \tag{10}$$

or

$$\begin{cases} \text{If } |P_1 - P_2| \bmod \alpha = 0 \text{ and } |P_3 - P_4| \bmod \alpha = 0 \\ \text{Then } |\pi(P_1) - \pi(P_3)| \bmod \alpha = 0 \\ \text{and } |\pi(P_2) - \pi(P_3)| \bmod \alpha = 0 \end{cases} \tag{11}$$

This worst case can be avoided if the interleaver satisfy the following mapping norm

$$\begin{cases} \text{If } |P_1 - P_2| \bmod \alpha = 0 \text{ and } |P_3 - P_4| \bmod \alpha = 0 \\ \text{Then } |\pi(P_1) - \pi(P_3)| \bmod \alpha \neq 0 \\ \text{and } |\pi(P_2) - \pi(P_4)| \bmod \alpha \neq 0 \end{cases} \tag{12}$$

or

$$\begin{cases} \text{If } |P_1 - P_2| \bmod \alpha = 0 \text{ and } |P_3 - P_4| \bmod \alpha = 0 \\ \text{Then } |\pi(P_1) - \pi(P_3)| \bmod \alpha \neq 0 \\ \text{and } |\pi(P_2) - \pi(P_3)| \bmod \alpha \neq 0 \end{cases} \tag{13}$$

As discussed earlier, not all sequences with a weight of 2 are bad. There is such a weight-4 sequence that don't incorporate formula (13) but they aren't considered as bad sequences. A threshold defined by a parameter in literature [12], which is given as follows:

$$12 + \left(k_1^{'} + k_2^{'} + k_3^{'} + k_4^{'}\right) + \left(Q_{\min} - 2\right) \le d_{\max}^{r=4} \tag{14}$$

$$\left(k_1^{'} + k_2^{'} + k_3^{'} + k_4^{'}\right) \le \frac{d_{\max}^{r=4} - 12}{Q_{\min-2}} \tag{15}$$

For a sequence declared as a bad weight-4 input sequence, it satisfies the inequalities in (10), (11), and (15) at the same time. Only if the input sequence doesn't satisfy one of the conditions, it will result in a bad sequence. In this paper, a turbo code with two identical RSC encoders in which generator polynomial $G(1,5/7)_8$ is used. The values of threshold parameters such as $d_{\max}^{r=2}$, $d_{\max}^{r=3}$, and $d_{\max}^{r=4}$ can be found in literature [12]. The parameters value $d_{\max}^{r=4} = d_{\max}^{r=2} = 20$, and $d_{\max}^{r=3} = 13$. For a particular code, the values $\alpha = 3$ and $Q_{\min} = 4$ are used. At the same time, let L_s be a design parameter which is an integer. The CMI must consider the S-random constraint of turbo code in literature [12]. Here, a random integer is defined, that is to say, any randomly selected numbers of bit is compared to the S previous randomly selected numbers of bit. If the difference of between them is less than S, it will ignore the currently selected integer and choose another value that satisfies the criterion during the algorithm process. The CMI will satisfy the criteria $S > L_s$ in this paper. Besides, we choose the value of L_S as $L_S = 17$ .To design CMI must map the criteria that were aforementioned in this section, we will take CMI and RI into an account with the proposed code cooperative scheme.

3. TC-DSM schemes for non-cooperation wireless system

The block diagram of TC-DSM scheme is presented in **Fig. 3**. The length of code is related to the number of transmitting antenna and 2^b-PSK constellation where b is an integer…. The turbo code considered in this article consists of two recursive systemic encoders (RSC). Each of the constituent RSCs is composed of a generator matrix $G_M = \left[1, g_a(D)/g_b(D)\right]$, where $g_a(D) = 1 + D^2$ is a forward polynomial and $g_b(D) = 1 + D + D^2$ is a backward polynomial.

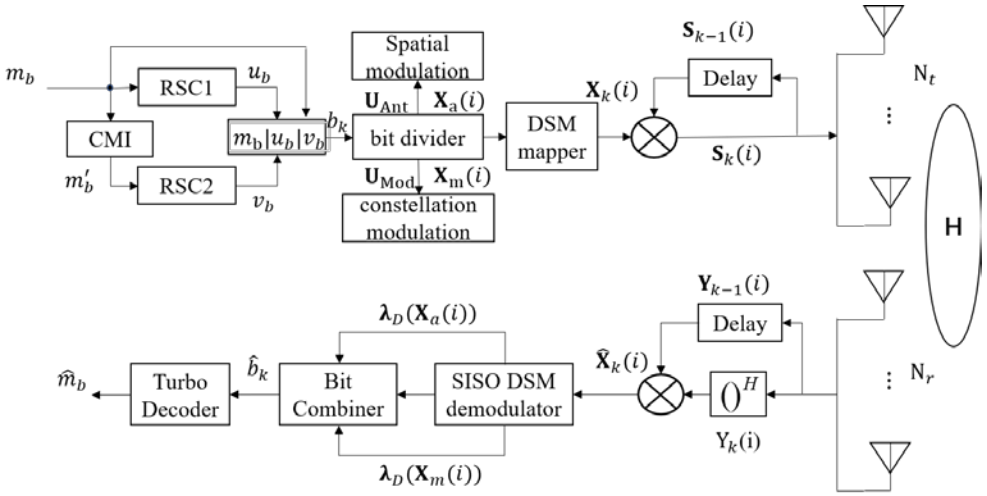

Fig. 3. Schematic of TC-DSM scheme for wireless communication system.

3.1 Transmission

3.1.1 The process of the signal transmission

In our proposed scheme, we first to design a DSM system in which N_t and N_r represents the number of transmit antennas and receive antennas, respectively. Suppose the symbol s_t is sent from the mth transmit antenna at time instant t, which can be denoted as $\mathbf{s} = \begin{bmatrix} 0 & \cdots & 0 & s_t & 0 & \cdots & 0 \end{bmatrix}^T$. The elements in $\mathbf{s}$ are zero vector except the mth entry s_t. Then, we collect the constellation vector $\mathbf{s}$ and form an $N_t \times N_t$ space–time block $\mathbf{S}$, that is the (m, t)th entry in block $\mathbf{S}$ indicates the symbol s_{mt} sent from transmit antenna m in time instant t. In the transmission process of DSM, each column and each row in $\mathbf{s}$ has exactly one non-zero entry. At the same time, the non-zeros are selected from to an equal energy 2^b-PSK alphabet A for some b=1,2,3…. That is to say, all the nonzero entries of $\mathbf{S}$ are selected from A. For example, a block for N_t=3 is given by $\mathbf{S} = \begin{bmatrix} 0 & s_{21} & 0 \\ 0 & 0 & s_{32} \\ s_{13} & 0 & 0 \end{bmatrix}$, which means that the symbols s_{13}, s_{21}, and s_{32} selected from A are transmitted from transmit antennas 3, 1, and 2 at time instants 1, 2, and 3, respectively. Simultaneously, the other two transmit antennas are free [22].

The DSM system needs to determine two steps: the first is to determine the spatial

information, that is, to determine the order of antenna activation in N_t time instants, and the second is to determine the symbol information. Let define a set ς include the whole possible space–time blocks **S**. Generally speaking, $2^{\lfloor \log_2(N_t!) \rfloor} 2^{N_t b}$ transmit blocks from ς should be choose and form a subset ς_M for de-mapping. Each transmit block can then be encoded with $\lfloor \log_2(N_t!) \rfloor + N_t b$ bits, where $\lfloor \log_2(N_t!) \rfloor$ symbols are used to determine the order of antenna activation in N_t time slots and $N_t * b$ symbols are used to determine the symbol information. Then the obtained new signal will be sent to perform a differential process, which will be depicted in later.

Then, we let m_b be the input sequence, and m_b be encoded to be turbo code b_k which comprising bits m_b and u_b , v_b , where m_b denotes a systematic bit, u_b and v_b denotes parity sequences respectively. Let N_t be the number of transmit antennas and N_r be the number of receive antennas. It should be mentioned that in the case of DSM [4, 14-16], the term $\lfloor \log_2(N_t!) \rfloor + N_t b$ is the spectral efficiency with 2^b-PSK constellation, which is represented by the symbol η [14] for some b=1,2,3…. If b_k is not a multiple of η, we will add some dummy bits to the sequence b_k , which will make the sequence b_k becomes a multiple of η. In this case, the detailed settings of turbo code for DSM based on different code lengths and constellation modulation is shown in **Table 1**. The sequence b_k must meet the requirement that the length N of b_k must be the integer multiple of η, where this system employs N_t transmitting antennas and 2^b-PSK constellation.

Table 1. Tailoring of turbo code for DSM

Parameters	**BPSK**		**QPSK**		**16-QAM**	
N	1024	2048	1024	2048	1024	2048
Dummy bits	1	2	0	0	12	10
Total block length	1025	2050	1024	2048	1036	2058
N_t	3	3	3	3	3	3
Added bits	5	5	8	8	14	14
Antenna bits	410	820	256	5122	148	294
Information bits	615	1230	768	136	888	1764
DSM symbols	205	410	128	256	74	147

The encoded turbo code sequence b_k is split to bit trains of length $W = \lfloor \log_2(N_t!) \rfloor + N_t b$, then allocate a transmitting antenna index to each bit train. Each bit train is marked L_t , (t$\in$(1: (length of b_k)/W) which include two binary sets, $\mathbf{U}_{Ant}$ and $\mathbf{U}_{Mod}$, where $\mathbf{U}_{Ant}$ represents the sequence selected by antenna (determine the order of antenna activation) and $\mathbf{U}_{Mod}$ represents the bits which is mapped to constitute constellation sequences (symbol information) as depicted in **Fig. 3**. The sequences $\mathbf{U}_{Ant}$ and $\mathbf{U}_{Mod}$ are sent to differential spatial mapper and constellation mapper blocks, respectively. The length of $\mathbf{U}_{Ant}$ is $\lfloor \log_2(N_t!) \rfloor$, and the sequences $\mathbf{U}_{Mod}$ are the remaining $N_t * b$ bits. Then, the transmitter encodes the bit stream b_k into bit trains L_t , (t$\in$(1: (length of b_k)/W) in a recursive manner.

Then, the differential transmission process will be performed next. The process of transmitting bit train begins the transmission with sending an arbitrary initial block $\mathbf{S}_0(i) \in \varsigma$,

as the 2^b-PSK constellation A contains symbol 1, we select $\mathbf{S}_0 = \mathbf{I}_{N_t}$ for any N_t without loss of generality. Suppose that from time $N_t(t-1)$ to $N_t t-1$, the (t-1)th block $\mathbf{S}_{t-1}$ is transmitted (t=1,2,3…) after the sequence b_k is spilt into some bit trains. Next, the operation of this encoding method during the space-time modulation is depicted as follows.

Step1: Given the input bit trains, firstly map one of it onto ς_M and obtain $\mathbf{X}_k(i) \in \varsigma_M \in \varsigma$. The first $\lfloor \log_2(N_t!) \rfloor$ bits $\mathbf{U}_{Ant}$ are mapped to spatial domain, which determines the order of transmit antennas selected in the space–time block through an index mapping method using a specific mapping algorithm (depicted in Section 3.1.1). Therefore, $\mathbf{u}_a(i) = [u_a(1), \cdots, u_a(k), \cdots u_a(I)]$ is the sequence determining the order of transmit antennas being activated, where $u_a(i) \in (1\text{:}\ N_t)$, $k \in (1\text{:}\ N_t)$. Further, the remaining $N_t * b$ bits $\mathbf{U}_{Mod}$ are sent to the signal domain, by which encoded into N_t constellation symbols. Therefore, $\mathbf{u}_m(i) = [u_m(1), \cdots u_m(k), \cdots u_m(I)]$ is the sequences decides symbol the transmitting antenna must send, where $u_m(i)$ is a symbol drawn from the 2^b-PSK constellation A and $k \in (1\text{:}N_t)$, $1 \le \mathrm{k} \le \mathrm{I}$. Taking into account the mapping results of both $\mathbf{U}_{Ant}$ and $\mathbf{U}_{Mod}$ the $\mathbf{X}_k(i)$ is get.

Step2: The transmitted block $\mathbf{S}_k(i)$ is set as:

$$\mathbf{S}_k(i) = \mathbf{S}_{(k-1)}(i)\mathbf{X}_k(i) \tag{16}$$

Note that given $\mathbf{S}_{(k-1)}(i)$ and $\mathbf{X}_k(i) \in \varsigma$, according to the literature [4], it is guaranteed that.

Step3: Send the block $\mathbf{S}_k$ during time period $N_t t$ to $N_t(t+1)-1$.

The given three-step process is iterated in the transmitted node until the whole bit trains is transmitted.

3.1.2 The manner of the index mapping

During the transmitting of a bit train, we use Lookup Table method to maps the first bits to the order for transmitting antennas being activated in a space–time block. Firstly, a lookup table is established to decide the corresponding permutations for the incoming $\mathbf{U}_{Ant}$ bits, whose length is $\lfloor \log_2(N_t!) \rfloor$. For example, N_t = 3 is showed

Table 2. Mapping table of lookup, N_t=3

Input bits	Activation sequence	Message block
00	(1 2 3)	$\begin{bmatrix} S_{11} & 0 & 0 \\ 0 & S_{22} & 0 \\ 0 & 0 & S_{33} \end{bmatrix}$
01	(1 3 2)	$\begin{bmatrix} S_{11} & 0 & 0 \\ 0 & 0 & S_{23} \\ 0 & S_{32} & 0 \end{bmatrix}$
10	(2 1 3)	$\begin{bmatrix} 0 & S_{12} & 0 \\ S_{21} & 0 & 0 \\ 0 & 0 & S_{33} \end{bmatrix}$
11	(2 3 1)	$\begin{bmatrix} 0 & 0 & S_{13} \\ S_{21} & 0 & 0 \\ 0 & S_{32} & 0 \end{bmatrix}$

3.2 Detection and decoding

From the time $N_t(t-1)$ to $N_t t-1$ the received information sequences are $\mathbf{Y}_{k-1}$ and $\mathbf{Y}_k$ respectively, which are modeled as,

$$\mathbf{Y}_{k-1}(i) = \mathbf{H}_{k-1}(i)S_{k-1}(i) + \mathbf{N}_{k-1}(i) \tag{17}$$

$$\mathbf{Y}_k(i) = \mathbf{H}_k(i)S_k(i) + \mathbf{N}_k(i) \tag{18}$$

where $\mathbf{Y}_{k-1}(i)$ and $\mathbf{Y}_k(i)$ is the received sequences over N_t successive time instants which represent the received sequences at receive antenna N at time instant t. $\mathbf{H}$ is the $N_r \times N_t$ channel matrix, which is independent and identically distributed complex Gaussian with zero mean and variance across antenna N and antenna M. The (N, M)th entry H_{NM} denotes the noise from transmitting antenna M to receive antenna N. The channel is assumed to be quasi-static and remain constant over $2N_t$ symbol durations. We can get (19) by using (16) and (17) into (18),

$$\mathbf{Y}_k(i) = \mathbf{Y}_{k-1}(i)\mathbf{X}_k(i) - \mathbf{N}_{k-1}(i)\mathbf{X}_k(i) + \mathbf{N}_k(i) \tag{19}$$

Thus, the maximum likelihood probability of detector be derived to

$$\hat{\mathbf{X}}_k(i) = \arg\max_{X \in G_M} trace[\mathrm{Re}(\mathbf{Y}_k^H(i)\mathbf{Y}_{k-1}(i)\mathbf{X}_k(i))] \tag{20}$$

Then get the decoded signals which are $N_r * N_t$ matrix. This particular SISO DSM demapper and turbo code decoder specify information processing flow of the receiver of the TC-DSM scheme. Let $\varphi_{l,0}$ and $\varphi_{l,1}$ be the subsets of antenna index which represent 0 and 1 at the l-th bit, respectively. Similarly, $\gamma_{l,0}$ and $\gamma_{l,1}$ represent the subsets of M-QAM symbol which have 0 and 1 at the l-th bit, respectively. Therefore, the log likelihood ratio (LLR) for the l-th bit of the antenna indexes and M-QAM symbol in TC-DSM is shown

$$\begin{aligned}\boldsymbol{\lambda}_D(u_a(i,l)) &= \log\frac{P(u_a(i,l)=0 \mid y_k(i))}{P(u_a(i,l)=1 \mid y_k(i))} \\ &= \log\frac{\sum_{\varphi}\sum_{\gamma_{i,0}} e^{-|Y_k(i)-hu_a(i)|^2+\sum_{\sigma=1}^{w}\log p(u_a,o(i))}}{\sum_{\varphi}\sum_{\gamma_{i,1}} e^{-|Y_k(i)-hu_a(i)|^2+\sum_{\sigma=1}^{w}\log p(u_a,o(i))}}\end{aligned} \tag{21}$$

$$\begin{aligned}\boldsymbol{\lambda}_D(u_m(i,l)) &= \log\frac{P(u_m(i,l)=0 \mid y_k(i))}{P(u_m(i,l)=1 \mid y_k(i))} \\ &= \log\frac{\sum_{\varphi}\sum_{\gamma_{i,0}} e^{-|Y_k(i)-hu_m(i)|^2+\sum_{\sigma=1}^{w}\log p(u_m,o(i))}}{\sum_{\varphi}\sum_{\gamma_{i,1}} e^{-|Y_k(i)-hu_m(i)|^2+\sum_{\sigma=1}^{w}\log p(u_m,o(i))}}\end{aligned} \tag{22}$$

These computed LLRs from (21) and (22) are collected and combined with bit combiner component that yields the soft bit sequence $\boldsymbol{\lambda}_D(U)$. This sequence is delivered to the turbo decoder which employs log-maximum a posterior probability (Log-MAP) decoding that eventually estimates the information bit sequence $\hat{m}_b$.

4. GDMTC-DSM Schemes

The distributed turbo code (DTC) scheme [15] can't be used for a strong fading channel condition as it has a weak RSC code between the source and relay node. Thence we choose GDMTC scheme that achieves a more superior signal path between the source and relay. The block diagram of GDMTC-DSM scheme is presented in **Fig. 4**. The source node in GDMTC-DSM scheme is different from the tradition turbo coded-cooperative scheme [16], which has two RSC in source node. This scheme is applied to any number of antennas (N_t, N_r).

The source node uses turbo code to encoder the information m_2 in the first time slot. Then DSM is performed over the obtained sequence u_1 i.e. $\mathbf{X}_m^S = u_1$ which has the codeword length $N_1 = N/2$. Therefore, the output sequence of coded DSM mapper $\mathbf{X}_{mu_1}^S(i_1) = [(x_{mu_1}^S(i_1^1), \cdots, x_{mu_1}^S(i_1^{N_t})]$ is transmitted to relay and destination node and $x_{mu_1}^S(i_1^n)$ is a column matrix and only one element of it is a M-QAM symbols, $m \in (1:M)$, $n \in (1:N_t)$, $i_1 \in (1:L_1)$, and L_1 is the length of the DSM sequence at the source node. During the time of slot 1, all the L_1 symbols in the sequence are then transmitted over the channel in turn.

During the time slot 1, the received sequence $\mathbf{Y}_{S,R}(i_1)$ at the relay node is shown as follow

$$\mathbf{Y}_{S,R}(i_1) = \mathbf{H}_{S,R}(i_1)\mathbf{X}_{mu_1}^S(i_1) + \mathbf{n}_{S,R}(i_1) \tag{23}$$

where $\mathbf{H}_{S,R}(i_1)$ is a $N_r \times N_t$ slow fading channel from source node to relay node. The fading coefficients of $\mathbf{H}_{S,R}(i_1)$ channel follows fading model Rayleigh. $\mathbf{n}_{S,R}(i_1)$ is an AWGN sequence, with which each element in it has a distribution of zero mean and $\mathbf{r}_{S,D}(i_1)$ variance per dimension.

Similarly, the received sequence $\mathbf{Y}_{S,D}(i_1)$ shown as

$$\mathbf{Y}_{S,D}(i_1) = \mathbf{H}_{S,D}(i_1)\mathbf{X}_{mu_1}^S(i_1) + \mathbf{n}_{S,D}(i_1) \tag{24}$$

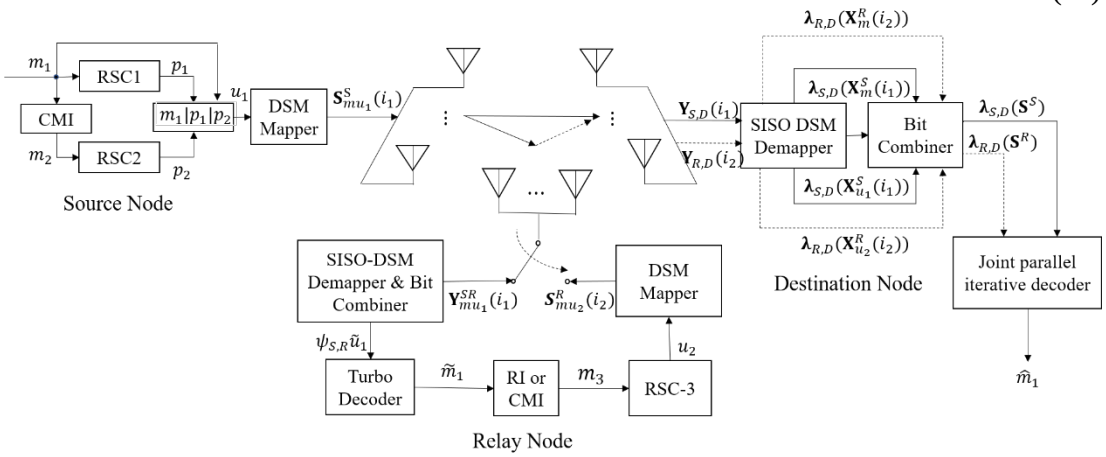

Fig. 4. Schematic of GDMTC-DSM scheme for wireless communication system.

where $\mathbf{H}_{S,D}(i_1)$ and $\mathbf{n}_{S,D}(i_1)$ are fading matrix and AWGN vector between source node and destination, respectively, which as the same to $\mathbf{H}_{S,R}(i_1)$ and $\mathbf{n}_{S,R}(i_1)$ in (23).

During the time slot 2, the received L_1 symbols $\mathbf{Y}_{S,R}(i_1)$ is be sent to DSM demapper and

combiner component to get the sequences $\boldsymbol{\lambda}_{S,R}\left(\mathbf{X}^S\right)$, the relay node firstly to demodulates it. The obtained soft sequences $\boldsymbol{\lambda}_{S,R}\left(\mathbf{X}^S\right)$ is transmitted to turbo decoder to get $\tilde{u}_1$. Then, the $\tilde{u}_1$ is interleaved using RI or CMI to get m_3. The relay node uses turbo code (m_3, p_3) to re-encode the m_3 information bits to get the parity code p_3 and the sequence u_2 which only include p_3. The codeword u_2 undergoes the encode of DSM, then the output sequence of DSM mapper $\mathbf{X}^R_{mu_2}(i_2)=[(x^R_{mu_2}(i_2^1),\ldots,x^R_{mu_2}(i_2^{N_t}))]$ is transmitted to destination node, where $X^R_{mu_2}(i_2^n)$ is the complex $2^{\boldsymbol{b}}$-PSK constellation symbol, $m\in(1:M)$, $n\in(1:N_t)$, $i_2\in(1:L_2)$ and $i_2\in(1:L_2)$ is the length of the DSM sequence at the relay node.

During the time slot 2, the received sequence at the destination node is shown

$$\mathbf{Y}_{R,D}(i_2)=\mathbf{H}_{R,D}(i_2)\mathbf{S}^S_{mu_2}(i_2)+\mathbf{n}_{R,D}(i_2) \tag{25}$$

where $\mathbf{H}_{R,D}(i_2)$ and $\mathbf{n}_{R,D}(i_2)$ are fading matrix and AWGN vector between source node and destination, respectively, which as the same to $\mathbf{H}_{S,R}(i_1)$ and $\mathbf{n}_{S,R}(i_1)$ in (24). Note that only the parity bit sequence p_3 is sent to the relay during the second time slot. The SISO-DSM demapper generates antenna select index LLRs $\boldsymbol{\lambda}_{S,D}\left(x^S_{u_1}(i_1)\right)$ and 2^b-PSK symbol LLRs $\boldsymbol{\lambda}_{S,D}\left(x^S_m(i_1)\right)$ against all the received $\mathbf{Y}_{S,D}(i_1)$ in the time slot 1. Similarly, the SISO-DSM demapper generates antenna select index LLRs $\boldsymbol{\lambda}_{S,D}\left(x^S_{u_2}(i_2)\right)$ and 2^b-PSK symbol LLRs $\boldsymbol{\lambda}_{S,D}\left(x^S_m(i_2)\right)$ against all the received $\mathbf{Y}_{S,D}(i_1)$ in the time slot 2. These LLRs symbol are combined in a same way as they were split during the transmission process by bit combiner. Then, the destination node demodulates all L_1 and L_2 received DSM symbols by SISO DSM demapper during their respective time slots. The overall code rate observed in this paper is $R_c^0=1/3$. Finally, the demodulated LLRs $\boldsymbol{\lambda}_{S,D}\left(\mathbf{X}^S_{u_1}(i_1)\right)$ and $\boldsymbol{\lambda}_{S,D}\left(\mathbf{X}^S_{u_1}(i_1)\right)$ are transmitting to joint turbo decoder to get the estimated information sequence $\hat{u}_1$.

Next, we will describe how the SISO DSM demapper and joint turbo decoder to decode the received sequences.

5. Joint parallel iterative decoding method for GDMTC-DSM scheme

The SISO DSM demapper performs the channel observation and uses (21) and (22) to generate LLR, as depicted in **Fig. 3**. The DSM demodulator estimates the soft bits $\boldsymbol{\lambda}_{S,D}\left(S^S_{u_1}(i_1)\right)$ for antenna index and soft bits $\boldsymbol{\lambda}_{S,D}\left(S^S_{m_1}(i_1)\right)$ for 2^{b}-PSK constellation symbols against the received noisy observation sequence $\mathbf{Y}_{S,D}(i_1)$. The way in which these soft bits are arranged and buffered in the bit combiner component is similar to the way they are divided into transmitting ends. The bit combiner component concatenates all the coded DSM modulation symbols and gives the soft bit turbo code sequence $\boldsymbol{\lambda}_{S,D}\left(\mathbf{X}^S\right)$. A similar operation is performed during the time slot 2 to generate a soft bit turbo code sequence $\boldsymbol{\lambda}_{R,D}\left(\mathbf{X}^R\right)$. Then

we send the LLRS $\boldsymbol{\lambda}_{S,D}\left(\mathbf{X}^{S}\right)$ and $\boldsymbol{\lambda}_{R,D}\left(\mathbf{X}^{R}\right)$ to parallel decoding block.

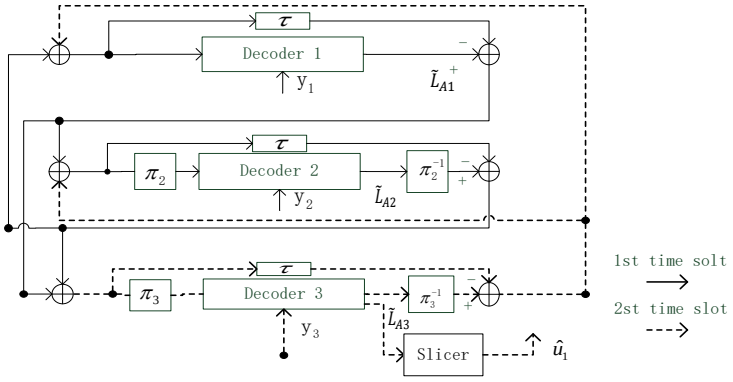

Fig. 5. Joint parallel iterative decoding method for GDMTC-DSM.

A parallel decoding scheme is proposed in literature [16], which can improve the code gain, and the author modifies because of the cooperative scenario for GDMTC. But this decoding scheme is very complicated and requires a lot of computing time when simulating it. Here we put forward a new parallel iterative decoding for GDMTC which also can improve the code gain with less complexity, which is shown as **Fig. 5**.

Let m_1 be the input information at the source, which can be encoded to a turbo code with N_1 codeword bits whose comprising bits are u_i, i=0,1,2, where u_0 denotes a systematic bit, u_2 and u_3 denotes parity sequences of p_1 and p_2 respectively. The corresponding received sequences at the destination are y_0, y_1 and y_2 respectively during the first time slot, where y_0 is the systematic component and is considered to be part of y_1.

During the second time slot, the relay encodes sequences A as a codeword y_3 and receives it as a sequence y_3 at the destination. Let us to assume all data bits have an equal prior probability, then, the best MAP decision metric for each bit can be shown in [16]:

$$L_A = \log\left(\frac{\sum_{m:m_k\approx 1} P\left(y_1/m\right)P\left(y_2/m\right)P\left(y_3/m\right)}{\sum_{m:m_k\approx 0} P\left(y_1/m\right)P\left(y_2/m\right)P\left(y_3/m\right)}\right) \tag{26}$$

However, (26) can't be computed for large interleaver size [19], and because of that y_2 and y_3 are not simple encodings of information bits with the two different interleaver π_2 and π_3.

But in this paper, we apply it to the calculation of the extrinsic information on decoding scheme. In Turbo code decoding, the external information bits correspond to the prior probability of information transmission. In a sense, external information is also equivalent to the information itself. We apply this formula for the computing of external information. Then we have

$$le_A = \log\left(\frac{\sum_{m:m_k\approx 1} P\left(y_1/m\right)P\left(y_2/m\right)P\left(y_3/m\right)}{\sum_{m:m_k\approx 0} P\left(y_1/m\right)P\left(y_2/m\right)P\left(y_3/m\right)}\right) \tag{27}$$

To compute $P\left(y_j \mid m\right)$, j=1,2,3 in (27), we get (28) with the Bayes' rule

$$P(le/y_i) \approx \prod_{A=1}^{N} \tilde{P}_i(le_A) \tag{28}$$

where l_e is equal to the value of extrinsic information. Let us define $\tilde{L}_{Aj}$ as follow

$$P_i(le_A) = \frac{e^{m_k \tilde{L}_{Aj}}}{1 + e^{m_k \tilde{L}_{Aj}}} \tag{29}$$

where $m_k \in \{0,1\}$. Then (27) can be represented by (30) for i=2,3 as follows

$$le_A = f(y_1, \tilde{L}_2, \tilde{L}_3, A) + \tilde{L}_{A2} + \tilde{L}_{A3} \tag{30}$$

where

$$f(y_1, \tilde{L}_2, \tilde{L}_3, A) = \log\left(\frac{\sum_{m:m_k \approx 1} P(y_1/m) P(y_2/m) P(y_3/m)}{\sum_{m:m_k \approx 0} P(y_1/m) P(y_2/m) P(y_3/m)}\right) \tag{31}$$

Again (27) also can be represented by (32) and (33) for i=1,3 as

$$le_A = f(y_2, \tilde{L}_1, \tilde{L}_3, A) + \tilde{L}_{A1} + \tilde{L}_{A3} \tag{32}$$

Similarly, for i=1,2 (27) can be given as

$$le_A = f(y_3, \tilde{L}_1, \tilde{L}_2, A) + \tilde{L}_{A1} + \tilde{L}_{A2} \tag{33}$$

A solution to eq. (30), (32) and (33) is given as

$$\begin{aligned} \tilde{L}_{A1} &= f(y_1, \tilde{L}_2, \tilde{L}_3, A) \\ \tilde{L}_{A2} &= f(y_2, \tilde{L}_1, \tilde{L}_3, A) \\ \tilde{L}_{A3} &= f(y_3, \tilde{L}_1, \tilde{L}_2, A) \end{aligned} \tag{34}$$

where k =1,2…N, N is the length of m_1. The end of decision depends on the output metric shown as follows

$$l_{e_A} = \tilde{L}_{A1} + \tilde{L}_{A2} + \tilde{L}_{A3} \tag{35}$$

which is also can be simply described as follows

$$l_{e_A} = \tilde{L}_{A3} \tag{36}$$

then it be sent to the slicer to get the final bit values of the message sequence $\hat{u}_1$.

We finally use the output information from the third decoder to make a hard verdict. We use it to the decoding of DMTC and get a better diversity gain.

6. Simulation results and discussion

Some comparisons are shown, for example, a comparison between the TC-DSM and GDMTC-DSM schemes impact of CMI and RI is presented. Besides, DSM is developed on the basis of SM. SM has applied rapidly to communication in recent years, we also applied these two communication schemes coded with SM that is called TC-SM and GDMTC-SM, which is in contrast to TC-DSM and GDMTC-DSM schemes, respectively. Moreover, we also provide comparisons between the impact on different number of receiving antennas between the two encoding proposals.

6.1 Performance comparisons between the schemes incorporating DSM and incorporating SM

The proposed schemes in the paper are simulated with slow Rayleigh fading channels. The generator matrix of turbo code is set to $G(1,5/7)_8$. The number of transmitting antennas is taken

as four or three and the number of transmit antennas are taken as four or three for all proposals. The modulation schemes chosen for this paper is BPSK. In our proposed schemes, the code rate is $R_c^0 = 1/3$. The CMI schemes will be compared with the RI schemes on different modulation schemes for BPSK. Further, we set an appropriate design rate, and we choose the length of code as 1024 bits and 2048 bits, respectively. The number of transmit antennas in all schemes is four, and the number of receiving antennas is four or three, respectively.

6.1.1 Performance comparisons between TC-SM and TC-DSM

Fig. 6 illustrates the BER of TC-SM and TC-DSM scheme over slow Rayleigh fading channel with a code length of 1024 bits. At the same time, **Fig. 7** illustrates the BER of TC-SM and TC-DSM scheme over slow Rayleigh fading channel with a code length of 2048 bits.

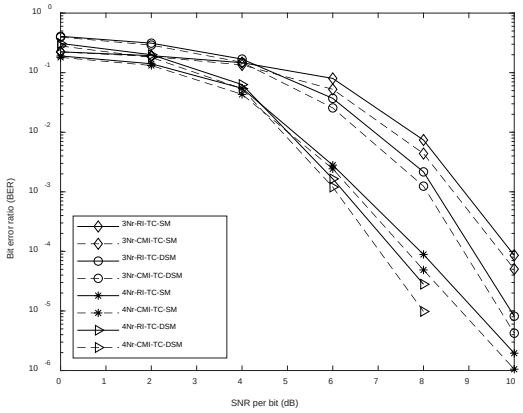

Fig. 6. The comparisons of BER performance between TC-DSM and TC-SM schemes over Rayleigh channel coded with BPSK for N=1024 bits and Nt=4, Nr=4 or Nr=3.

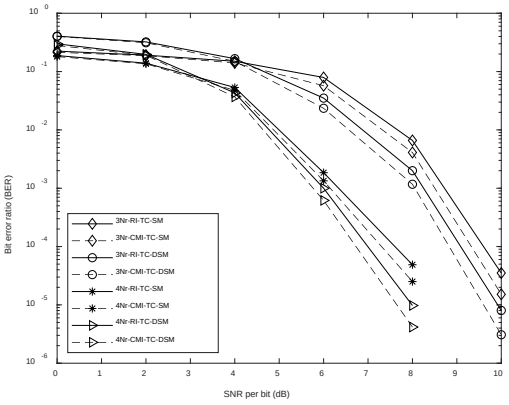

Fig. 7. The comparisons of BER performance between TC-DSM and TC-SM schemes over Rayleigh channel for N=2048 bits and N_t=4, N_r=4 or N_r=3.

From the two figures we can get the considered TC schemes incorporating CMI clearly outperforms RI schemes with BPSK modulation over slow Rayleigh fading channel. The considered scheme incorporating CMI evidently has a better BER performance in medium to high SNR regime by 0.3dB. Besides, the waterfalls region exhibits steeper slope because of that the CMI ensures that there are no short cycle events occurred. It was observed that the

scheme cooperative DSM clearly outperforms its counterpart cooperative SM scheme in SNR regime of 4-10 dB. As depicted in **Fig. 6**, the schemes incorporating DSM with the N_r=3 achieve 0.8 dB gain relative to its counterpart incorporating SM schemes in SNR regime of 4-10 dB, while the schemes incorporating DSM with N_r=4 achieve 1 dB gain relative to its counterpart incorporating SM schemes.

Moreover, the considered schemes with the length of 2048 bits as shown in **Fig. 7** has similar performance as shown in **Fig. 6**, but the BER is lower than the considered schemes with the length of 1024 bits. In this case of N_r=4, the BER value of considered scheme with RI coded cooperative DSM with the length of 2048 bit has come to 0 when the value of SNR is 10 dB, while the its counterpart scheme with the length of 1024 bits at the BER of 8×10^{-6}. We can find that the higher the number of receive antennas, the better the BER performance of our proposed scheme. Similarly, the longer the length of the information codeword, the better the BER performance of our proposed scheme.

6.1.2 Performance comparisons between GMDTC-SM and GMDTC-DSM

Fig. 8 illustrates the BER of GMDTC-SM and GMDTC-DSM schemes over slow Rayleigh fading channel with a code length of 1024 bits. **Fig. 9** illustrates the BER of GMDTC-SM and GMDTC-DSM scheme over slow Rayleigh fading channel with a code length of 2048 bits. The proposed schemes all are coded in BPSK.

It can be seen that the considered GMDTC scheme incorporating CMI also clearly outperforms RI in BPSK, but the SNR gain of the schemes incorporating CMI compared to the schemes incorporating RI are not equal under different number of receive antenna. It was observed that the cooperative DSM scheme outperforms its counterpart cooperative SM scheme in SNR regime of 2-10 dB. As depicted in **Fig. 8**, the schemes incorporating DSM with the Nr=3 achieve roughly 2 dB gain relative to its counterpart incorporating SM schemes in SNR regime of 10-14 dB, while the schemes incorporating DSM with the Nr=4 achieve 1 dB gain relative to its counterpart incorporating SM schemes under the value of SNR is 6 dB. As the SNR increases, the BER of GMDTC-DSM scheme with Nr=4 is getting to 0 dB as SNR=8 dB, while the BER of GMDTC-DSM scheme with Nr=3 is getting to 0 dB as SNR= 12 dB. At the same time, the performance of schemes with the length of 2048 bits as shown in **Fig. 9** also has similar performance as shown in **Fig. 8**, but the BER is lower than the considered schemes with the length of 1024 bits. In this case of N_r=4, the BER of considered scheme with RI coded cooperative DSM with the length of 2048 bit at the BER of 1.3×10^{-4} when the value of SNR is 8 dB, while the its counterpart scheme with the length of 1024 bits at the BER of 2.3×10^{-4}.

We also can see that the higher the number of receive antennas, the better the BER performance of our proposed scheme. Similarly, the longer the length of the information codeword, the better the BER performance of our proposed scheme. We can get that the GMDTC-DSM scheme is better than the GMDTC-SM scheme in terms of BER performance from **Fig. 8** and **Fig. 9**. Similarly, the GMDTC-DSM scheme is better than the TC-DSM scheme in terms of BER performance from **Fig. 6** to **Fig. 9**.

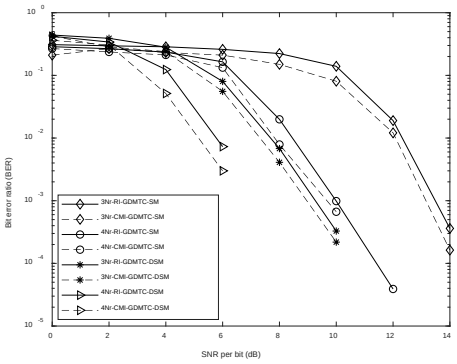

Fig. 8. The comparisons of BER performance between GMDTC-DSM and GMDTC-SM schemes over Rayleigh channel for N=1024 bits and N_t=4, N_r=4 or N_r=3.

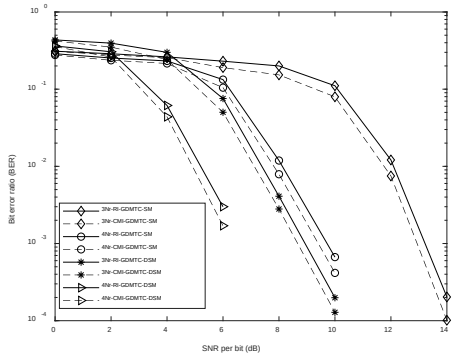

Fig. 9. The comparisons of BER performance between GMDTC-DSM and GMDTC-SM schemes over Rayleigh channel for N=2048 bits and N_t=4, N_r=4 or N_r=3.

6.2 Performance comparisons of the schemes coded-cooperative DSM

The modulation schemes chosen for this paper are BPSK, QPSK, and 16-QAM, respectively. In our proposed schemes, the code rate is $R_c^0 = 1/3$.The spectral efficiencies of proposed DSM scheme for BPSK, QPSK and 16-QAM schemes are 2, 4 and 6 b/s/Hz, respectively. The CMI schemes will be compared with the RI schemes on different schemes for BPSK, QPSK, and 16-QAM. The number of transmit antennas in all schemes is three, and the number of receiving antennas is two or three, respectively.

6.2.1 Performance comparisons for TC-DSM

Fig. 10 and **Fig. 11** illustrates the BER of TC-DSM scheme over slow Rayleigh fading channel with a code length of 1024 bits and 2048 bits, respectively. It can be seen from the two figures that compared with higher-order modulation that is only useful when the SNR is high enough, and the lower order modulation can only be useful when the SNR is sufficiently high, the lower order modulation is more flexible and can tolerate more noise interference. The proposed TC-DSM with CMI scheme clearly outperforms TC-DSM with RI scheme in different modulations, as depicted in **Fig. 10** and **Fig. 11**. The CMI scheme gets roughly 0.6 dB better performance than the RI scheme at the BER of 10^{-4}. At the same time, the scheme for N_r=3 achieves a better error performance than the scheme for N_r=2. The scheme incorporating N_r=3 achieves an improvement approximately 5dB relative to the schemes incorporating N_r=2 at BER of 10^{-2} in **Fig. 10** and **Fig. 11**.

Fig. 10 illustrates the BER of TC-DSM scheme over slow Rayleigh fading channel for length of code is 1024 bits. The digital modulation techniques are the same with before. It shows that CMI gets an improvement of 1dB relative to RI at BER of 10^{-5} when compares the simulation results for the TC-DSM in BPSK modulation for N_r=3. The BER of the TC-DSM scheme for N_r=3 based on BPSK modulation incorporating CMI when SNR is 9dB reaches to 10^{-5}, then reduces to zero in higher SNR. The BER of the TC-DSM scheme for N_r=3 based on QPSK modulation incorporating CMI when SNR value is 12dB reaches to 10^{-3}, then reduces to zero in higher SNR. The BER of the TC-DSM scheme for N_r=3 based on 16QAM modulation incorporating CMI when SNR value is reaches to 10^{-4}, then reduces to zero in higher SNR.

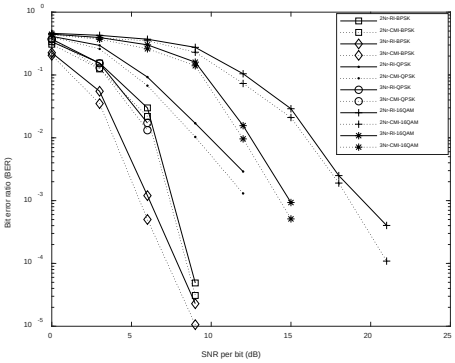

Fig. 10. BER performance of TC-DSM scheme over Rayleigh channel for N=1024 bits and N_r=3, or N_r=2.

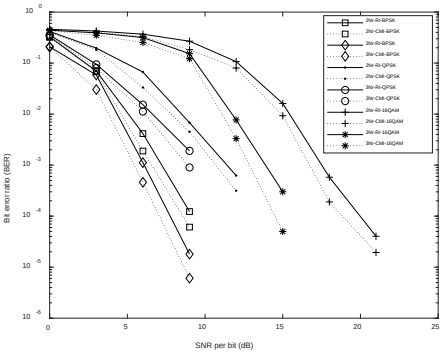

Fig. 11. BER performance of TC-DSM scheme over Rayleigh channel for N=2048 bits and N_r=3, or N_r=2.

Fig. 11 illustrates the BER of TC-DSM scheme over slow Rayleigh fading channel with a length of 2048 bits. The CMI also gets a better performance than RI in high SNR. The scheme for N_r=3 achieves a better BER performance than the scheme for N_r=2, just like the case when the code length as 1024 bits. The scheme for N_r=3 achieves about 5 dB gains in SNR relative to the scheme with N_r=2 at the BER of 10^{-4}. The BER of the TC-DSM scheme for N_r=3 based on BPSK modulation incorporating CMI when SNR is 9dB reaches to $5*10^{-5}$, then reduces to zero in higher SNR. The BER of the TC-DSM scheme for N_r=3 based on QPSK modulation incorporating CMI when SNR is 9dB reaches to 10^{-3}, then it reduces to zero in higher SNR. The BER of the TC-DSM scheme for N_r=3 based on 16-QAM modulation incorporating CMI when SNR is 10dB is about 10^{-5}, then it reduces to zero in higher SNR. We can see that the

BER performance of the code length of 2048 scheme is better than that of the code length of 1024 schemes for almost SNR values.

6.2.2 Performance comparisons for GMDTC-DSM

In this section, **Fig. 12** illustrates the BER of GDMTC-DSM scheme over slow Rayleigh fading channel for length of code is 1024 bits. At the same time, **Fig. 13** illustrates the BER of GDMTC-DSM scheme with a code length of 2048 bits.

These two figures also show that higher-order modulation (such as 16QAM) also outperforms the low-order modulation (such as BPSK) in the GDMTC-DSM scheme, which is the same with the scheme for TC. It also can be seen that the BER performance of the GDMTC-DSM with CMI is better than RI in these modulations over fading channels, and the CMI achieves an improvement in 0.6 dB relative to RI at the BER of 10^{-4}. At the same time, the scheme for N_r=3 achieves a better performance than the scheme for N_r=2 in two figures.

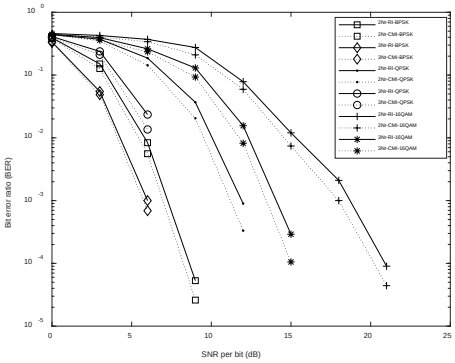

Fig. 12. BER performance of GDMTC-DSM scheme over Rayleigh channel N=1024 bits and N_t=3, N_r=2.

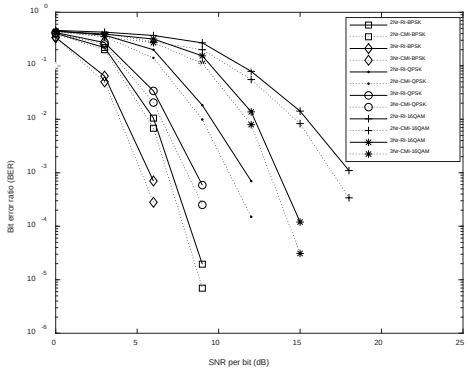

Fig. 13. BER performance of GDMTC-DSM scheme over Rayleigh channel N=2048 bits and N_t=3, or N_r=2.

Fig. 12 illustrates the BER of GDMTC-DSM scheme over slow Rayleigh fading channel for length of code is 1024 bits. The BER of the GDMTC-DSM scheme for N_r=3 based on BPSK modulation incorporating CMI when SNR is 9dB reaches to $3*10^{-3}$, then reduces to zero in higher SNR. The BER of the GDMTC-DSM scheme for N_r=3 based on QPSK modulation incorporating CMI when SNR is 6dB reaches to 10^{-3}, then reduces to zero in higher SNR. The BER of the GDMTC-DSM scheme for N_r=3 based on 16-QAM modulation incorporating CMI when SNR is 15dB reaches to 10^{-4}, then it reduces to zero in higher SNR.

The figure shows the GDMTC-DSM scheme gets a better BER performance than the TC-DSM scheme.

Fig. 13 illustrates the BER of GDMTC-DSM scheme over slow Rayleigh fading channel. The BER performance of the considered scheme incorporating CMI outperforms RI in each modulation over fading channels, and the CMI achieves an improvement in 0.6 dBs relative to RI at the BER of 10^{-3}. The BER of the GDMTC-DSM scheme for N_r=3 based on BPSK modulation incorporating CMI when SNR is 6dB reaches to $6*10^{-3}$, then reduces to zero in higher SNR. The BER of the GDMTC-DSM scheme for N_r=3 based on QPSK modulation incorporating CMI when SNR is 9dB reaches to $6*10^{-3}$, then reduces to zero in higher SNR. The BER of the GDMTC-DSM scheme for N_r=3 based on 16-QAM modulation incorporating CMI when SNR is 15dB reaches to $7*10^{-4}$, then reduces to zero in higher SNR.

From the four figures we get that the coded cooperative GDMTC-DSM communication scheme outperforms the TC-DSM communication scheme. For example, when the length of code is 2048 bits and N_r=3, the BER of the TC scheme based on BPSK incorporating CMI when SNR is 9dB reaches to $2.2*10^{-5}$, while the BER of the GDMTC-DSM scheme based on BPSK incorporating CMI have reduced to zero. Finally, the scheme incorporating CMI is better than RI in each modulation through fading channels, which due to the CMI could increase the minimum free distance of the turbo code.

6.3 Performance comparisons between the GDMTC-DSM and other scheme

The literature [27] proposed a coded spatial modulation scheme based on polar code, which is called MLPCC−SM scheme. We compare the performance of GDMTC-DSM scheme with its performance here. The number of transmit and receive antennas all is four. **Fig. 14** illustrates the comparison results of GDMTC-DSM scheme and MLPCC-SM scheme over slow Rayleigh fading channel.

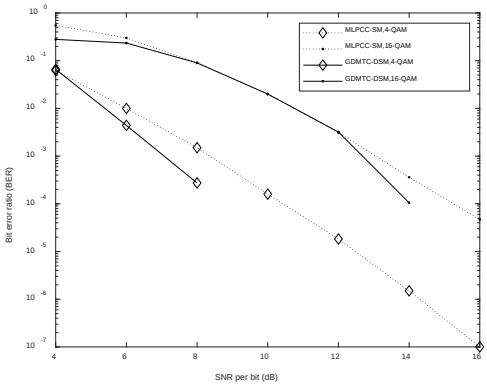

Fig. 14. BER performance of GDMTC-DSM scheme and MLPCC-SM scheme over Rayleigh channel and Nt=4, Nr=4.

The BER performance of the GDMTC-DSM scheme outperforms MLPCC-SM in 4-QAM or 16-QAM modulation over Rayleigh fading channels. The BER of the GDMTC-DSM scheme based on 16-QAM modulation reaches to $1*10^{-4}$ when SNR is 14dB, then reduces to zero in higher SNR. The BER of the GDMTC-DSM scheme based on 4-QAM modulation reaches to $2.7*10^{-4}$ when SNR is 8dB, then reduces to zero in higher SNR. The performance of GDMTD-DSM scheme has advantages over MLPCC-SM.

7. Conclusion

Here we proposed a scheme for wireless communication system which named GDMTC-DSM. At the same time, we proposed a joint parallel iterative decoding method for GDMTC-DSM scheme, which get an effective gain over fading channels. The performance of the CMI is discussed on the two schemes. In addition, the schemes incorporating CMI are better than the schemes incorporating RI scheme in each modulation on the fading channel. At the same time, the GDMTC-DSM scheme and the TC-DSM scheme gets a better performance than the GDMTC-SM scheme and TC-SM scheme, respectively. Further, the coded cooperative DSM scheme gets a better performance in coding gain, diversity gain, and cooperation gain successfully than non-cooperative scheme. In addition, the scheme incorporating three receiving antennas achieves more gain than the scheme incorporating two receiving antennas. A large number of antennas can be deployed at the destination to further reduce the probability of error. Therefore, it is feasible to deploy more DSM antennas in a distributed, multi-cooperative, and diversified manner, and it is very promising for the future communication technology.

References

[1] S. Alamouti, “A simple transmit diversity technique for wireless communications,” *IEEE J. Sel. Areas Commun*., vol. 16, pp. 1451–1458, 1998. Article (CrossRef Link)
[2] M. Wen, Q. Li, E. Basar, et al., “Generalized multiple-mode OFDM with index modulation,” *IEEE Transactions on Wireless Communications*, 17(10), 6531-6543, 2018. Article (CrossRef Link)
[3] J. Li, S. Dang, M. Wen, et al., “Layered Orthogonal Frequency Division Multiplexing with Index Modulation,” *IEEE Systems Journal*, 13(4), 3793-3802, 2019. Article (CrossRef Link)
[4] R. Y. Mesleh, H. Haas, S. Sinanovic, C.W. Ahn, & S. Yun, “Spatial modulation. *IEEE Transactions on Vehicular Tech-nology*, 57(4), 2228–2241, 2008. Article (CrossRef Link)
[5] D. Ma, N. Shlezinger, T. Huang, et al., “Spatial Modulation for Joint Radar-Communications Systems: Design, Analysis, and Hardware Prototype,” *IEEE Transactions on Vehicular Technology*, 70(3), 2283-2298, 2021. Article (CrossRef Link)
[6] J. Li, M. Wen, C. Xiang, et al., “Generalized Precoding-Aided Quadrature Spatial Modulation,” *IEEE Transactions on Vehicular Technology*, 66(2), 1881-1886, 2017. Article (CrossRef Link)
[7] M. Wen, B. Zheng, K.J. Kim, et al., “A Survey on Spatial Modulation in Emerging Wireless Systems: Research Progresses and Applications,” *IEEE Journal on Selected Areas in Communications*, 37(9), 1949-1972, 2019. Article (CrossRef Link)
[8] Y. Bian, C. Xiang, M. Wen, et al., “Differential Spatial Modulation,” *IEEE Transactions on Vehicular Technology*, 64(7), 3262-3268, 2015. Article (CrossRef Link)
[9] L. Xiao, Y. Xiao, P. Yang, et al., “Space-Time Block Coded Differential Spatial Modulation,” *IEEE Transactions on Vehicular Technology*, 66(10), 8821-8834, 2017. Article (CrossRef Link)
[10] J. Li, M. Wen, X. Cheng, et al., “Differential Spatial Modulation with Gray Coded Antenna Activation Order,” *IEEE Communications Letters*, 20(6), 1100-1103, 2016. Article (CrossRef Link)
[11] D. Yu, G. Yue, A. Liu, et al., “Absolute Amplitude Differential Phase Spatial Modulation and Its Non-Coherent Detection Under Fast Fading Channels,” *IEEE Transactions on Wireless Communications*, 19(4), 2742-2755, 2020. Article (CrossRef Link)
[12] D. Wang, L. Hao, “Performance analysis for cooperative relay communication,” *Wirel. Pers. Commun*., 71, 1619–1631, 2013. Article (CrossRef Link)
[13] T.E. Hunter, A. Nosratinia, “Diversity through code cooperation,” *IEEE Trans. Wirel. Commun*., 5(2), 283–289, 2006. Article (CrossRef Link)
[14] A. Sendonaris, E. Erkip, B. Aazhang, “User cooperation diversity. Part I. System description,” *IEEE Trans. Communication*, 51(11), 1927–1938, 2003. Article (CrossRef Link)

[15] A. Sendonaris, E. Erkip, B. Aazhang, "User cooperation diversity. Part II. System description," *IEEE Trans. Commun*., 51(11), 1927–1938, 2003. Article (CrossRef Link)
[16] B. Zhao and M. C. Valenti, "Distributed turbo coded diversity for relay channel," *Electron. Lett*., vol. 39, pp. 786–787, 2003. Article (CrossRef Link)
[17] X. Jin, Q. Li, N. Jin, et al., "Design of Differential Spatial Modulation Cooperative System Based on Complementary Code," *Wireless Personal Communications*, 111(4), 1475-1476, 2020. Article (CrossRef Link)
[18] B. Tahir, S. Schwarz, and M. Rupp, "BER comparison between convolutional, turbo, LDPC, and polar codes," in *Proc. of 2017 24th International Conference on Telecommunications (ICT)*, IEEE, pp. 1–7, 2017. Article (CrossRef Link)
[19] L. Xiang, M. F. Brejza, R. G. Maunder, B. M., "Al-Hashimi, and L. Hanzo, "Arbitrarily parallel turbo decoding for ultra-reliable low latency communication in 3GPP LTE," *IEEE Journal on Selected Areas in Communications*, vol. 37, no. 4, pp. 826–838, 2019. Article (CrossRef Link)
[20] Y. Liu, L. Xiang, R, G. Maunder, et al., "Hybrid Iterative Detection and Decoding of Near-Instantaneously Adaptive Turbo-Coded Sparse Code Multiple Access," *IEEE Transactions on Vehicular Technology*, 2021.
[21] S. Ejaz, F.F. Yang, "Turbo Codes with Modified Code Matched Interleaver for Coded-Cooperation in Half-Duplex Wireless Relay Networks," *Frequenz*, 69(3-4), 171-184, 2015. Article (CrossRef Link)
[22] J. Ramsey, "Realization of optimum interleavers," *Information Theory IEEE Transactions on*, 16(3), 338-345, 1970. Article (CrossRef Link)
[23] F. Wen, J. Yuan, and B. S., Vucetic, "A code-matched interleaver design for turbo codes," *IEEE Trans. Commun*., vol. 50, pp. 926–937, 2002. Article (CrossRef Link)
[24] D. Divsalar, F. Pollara, "Multiple turbo codes," in *Proc. of IEEE Military Communications Conference*, IEEE, 279-285, 1995. Article (CrossRef Link)
[25] D. Divsalar and F. Pollara, "Turbo codes for PCS applications," in *Proc. of 1995 IEEE Int. Conf. on Communications, 1995, ICC'95 Seattle, 'Gateway to Globalization'*, pp. 54–59, 1995. Article (CrossRef Link)
[26] Berrou C, Glavieux A, "Near optimum error correcting coding and decoding: Turbo-codes," *IEEE Transactions on Communications*, 44(10), 1261-1271, 1996. Article (CrossRef Link)
[27] Mughal S, Yang F, Xu H, et al., "Coded cooperative spatial modulation based on multi-level construction of polar code," *Telecommunication Systems*, 70, 435-446, 2019. Article (CrossRef Link)

Jiangli Zeng was born in 1989. She received the B.S. degree in communication engineering from Ningxia University, Ningxia, China, in 2012, and the M.Sc. in Circuits and Systems from the Ningxia University in 2015. She is currently pursuing the Ph.D. degree with the College of Electronics and Information Engineering, Nanjing University of Aeronautics and Astronautics, Nanjing, China. Her current research interests include information theory, channel coding, cooperation communication and differential spatial modulation and their applications to wireless communication.

Sanya Liu was born in 1988. She received the B.S. degree in communication engineering from Binzhou University, Binzhou, China, in 2011; the M.S. degree in electronics and communication engineering from Ningxia University, Ningxia, China, in 2014; and the Ph.D. degree from Xiamen University, Xiamen, China, in 2021. She is currently an assistant professor with the School of Communication Engineering at the Huaqiao University. Her current research interests include information theory, source coding, joint source and channel coding and their applications to wireless communication, and image processing.

Hui Wang was born in 1989. In 2011, she received a bachelor's degree in communication engineering from Binzhou University, Shandong Province, China, and a master's degree in communication and information systems from Civil Aviation University of China, Tianjin, China, in 2014. She currently works in the equipment information room of Wenzhou Air Traffic Management Station of Civil Aviation of China. Her current research interests include information theory, source coding.